Eur. Phys. J. C 50, 771–779 (2007)
DOI 10.1140/epjc/s10052-007-0245-3

THE EUROPEAN PHYSICAL JOURNAL C

Regular Article – Theoretical Physics

Determination of the η and η' mixing angle from the pseudoscalar transition form factors

Tao Huang[1,a], Xing-Gang Wu[2,3,b]

[1] Institute of High Energy Physics, Chinese Academy of Sciences, P.O. Box 918(4), Beijing 100039, P.R. China
[2] Institute of Theoretical Physics, Chinese Academy of Sciences, P.O. Box 2735, Beijing 100080, P.R. China
[3] Department of Physics, Chongqing University, Chongqing 400044, P.R. China

Received: 1 December 2006 /
Published online: 13 March 2007 –

Abstract. The possible range of the η–η' mixing angle is determined from the transition form factors $F_{\eta\gamma}(Q^2)$ and $F_{\eta'\gamma}(Q^2)$ with the help of up-to-date experimental data. For this purpose, the quark-flavor mixing scheme is adopted and the pseudoscalar transition form factors are calculated in the framework of light-cone pQCD, in which the transverse-momentum corrections and the contributions beyond the leading Fock state have been carefully taken into consideration. We construct a phenomenological expression to estimate the contributions to the form factors beyond the leading Fock state, based on their asymptotic behavior at $Q^2 \to 0$ and $Q^2 \to \infty$. By taking the quark-flavor mixing scheme, our results lead to $\phi = 38.0^\circ \pm 1.0^\circ \pm 2.0^\circ$, where the first error comes from the experimental uncertainty and the second error from the uncertainties of the parameters of the wavefunction. The possible intrinsic charm component in η and η' is discussed, and our present analysis also disfavors a large intrinsic charm component in η and η', e.g. $|f^c_{\eta'}| \leq 50$ MeV.

PACS. 13.40.Gp; 12.38.Bx; 14.40.Aq

1 Introduction

The light-cone (LC) formalism [1–4] provides a convenient framework for the relativistic description of hadrons in terms of quark and gluon degrees of freedom and for the application of pQCD to exclusive processes. Among these, η–η' mixing is a subject of considerable interest, which has been examined in many investigations, i.e. experimental ones [5–15] and theoretical ones [16–26]. Some experiments have been done recently, e.g. the new KLOE value of $R_\phi = \frac{\Gamma[\phi\to\eta'\gamma]}{\Gamma[\phi\to\eta\gamma]} = (4.9 \pm 0.1_{\rm stat} \pm 0.2_{\rm syst}) \times 10^{-3}$ [11] leads to $\phi = 41.2^\circ \pm 1.2^\circ$ [14]; the BES collaboration has announced a new measured value for $R_{J/\Psi}$, i.e. $R_{J/\Psi} = \frac{\Gamma[J/\Psi\to\eta'\gamma]}{\Gamma[J/\Psi\to\eta\gamma]} = 4.94 \pm 0.40$ [15], which leads to $\phi = 38.8^\circ \pm 1.2^\circ$. Furthermore, new measurements of the form factors $F_{\eta\gamma}(Q^2)$ and $F_{\eta'\gamma}(Q^2)$ in the asymptotic region by the BaBar collaboration [12], $Q^2 F_{\eta\gamma}(Q^2)|_{Q^2=112\ {\rm GeV}^2} = 0.229 \pm 0.030 \pm 0.008\,{\rm GeV}$ and $Q^2 F_{\eta'\gamma}(Q^2)|_{Q^2=112\ {\rm GeV}^2} = 0.251 \pm 0.019 \pm 0.008\,{\rm GeV}$, will provide further constraints on the theoretical predictions.

The pseudoscalar transition form factors $F_{\eta\gamma}(Q^2)$ and $F_{\eta'\gamma}(Q^2)$ provide a good platform to study η and η' mixing effects; these have already been studied in the literature by several groups [22–24, 27–29]. However, in these calculations, either only the leading Fock state (see e.g. [28]) or only the asymptotic behavior of the form factors (see e.g. [29]) have been taken in consideration to determine the mixing angle. As has been pointed out in [24, 27], the mixing angle cannot be reliably determined without properly considering the contributions from the non-valence quark states, due to the fact that even though the contributions of the higher Fock states are power suppressed in a large Q^2 region, they will give sizable contributions to the small and intermediate regions. In fact, it has been pointed out in [30, 31] that the leading Fock state contributes only half of $F_{P\gamma}(Q^2)|_{Q^2=0}$ (P stands for the pseudoscalar mesons), and the remaining half should come from the higher Fock states. The contributions of higher Fock states in a small Q^2 region cannot be calculated in the perturbative QCD approach due to its non-perturbative features. Recently, the authors of [32] have constructed a phenomenological expression for the pion–photon transition form factor to estimate the contributions beyond the leading Fock state, based on its asymptotic behavior at $Q^2 \to 0$ and $Q^2 \to \infty$ (Q^2 stands for the momentum transfer in the process). These predicted results for $F_{\pi\gamma}(Q^2)$ agree well with the experimental data in the whole Q^2 region. In the present paper, we will adopt this newly developed method to estimate the higher Fock state contributions of the form factors $F_{\eta\gamma}(Q^2)$ and $F_{\eta'\gamma}(Q^2)$ and then to derive the possible

[a] e-mail: huangtao@mail.ihep.ac.cn
[b] e-mail: wuxg@itp.ac.cn

range for the mixing angle by comparing the predicted results with the experimental data.

As for η–η' mixing, two mixing schemes are adopted in the literature, i.e. the octet–singlet mixing scheme and the quark-flavor mixing scheme. These two schemes can be related to a proper rotation of the ideal mixing angle ($\theta_{\rm id} = -\arctan\sqrt{2} \simeq -54.7^\circ$) [21, 33]. A dramatic simplification can be achieved by adopting the quark-flavor mixing scheme; especially, the decay constants in the quark-flavor basis simply follow the pattern of state mixing due to the OZI-rule [21]. Furthermore, by adopting the quark-flavor mixing scheme and also by carefully dealing with the higher Fock state contributions, a naive discussion (at the end of Sect. 2.3) shows that the value of $Q^2F_{\eta\gamma}(Q^2)$ decreases, while the value of $Q^2F_{\eta'\gamma}(Q^2)$ increases, with increasing mixing angle ϕ, so the possible range for ϕ can be derived by comparing with the experimental data on the form factors $F_{\eta\gamma}(Q^2)$ and $F_{\eta'\gamma}(Q^2)$. And then, by adopting the relation between the two schemes as shown in [21, 33], all the three mixing angles θ_P, θ_1 and θ_8 involved in the octet–singlet scheme can be determined, where θ_P is the mixing angle for the states and the $\theta_{1/8}$ are the mixing angles for the decay constants f_1 and f_8. The theoretical and phenomenological considerations performed in [19, 22, 34, 35] also favor the quark-flavor basis. Therefore, we will adopt the quark-flavor mixing scheme to do our calculation throughout the paper.

The paper is organized as follows. In Sect. 2, we outline our techniques for determining the η–η' mixing angle, in which expressions for the pseudoscalar transition form factors beyond the leading Fock state are provided. In Sect. 3, we present the numerical results for the $\eta\gamma$ and $\eta'\gamma$ transition form factors, and then we derive the possible range for the mixing angle ϕ by comparing with the present experimental data on the form factors $F_{\eta\gamma}(Q^2)$ and $F_{\eta'\gamma}(Q^2)$. Some discussion of the uncertainty sources for ϕ determination is provided in Sect. 4. The final section is reserved for our summary.

2 $\eta - \eta'$ mixing angle and expressions of the pseudoscalar transition form factors beyond the leading Fock state

2.1 Definition in the quark-flavor basis

In the quark-flavor basis, the two orthogonal basis states are assumed to have the following parton composition in the Fock state description:

$$|\eta_q\rangle = \Psi_{\eta_q}\frac{|u\bar{u}+d\bar{d}\rangle}{\sqrt{2}} + \cdots, \quad |\eta_s\rangle = \Psi_{\eta_s}|s\bar{s}\rangle + \cdots, \quad (1)$$

where the Ψ_{η_i} $(i = q, s)$ denote the LC wavefunctions of the corresponding parton states, and the dots stand for higher Fock states. The physical meson states are related to the basis (1) by an orthogonal transformation,

$$\begin{pmatrix}|\eta'\rangle\\|\eta'\rangle\end{pmatrix} = U(\phi)\begin{pmatrix}|\eta_q\rangle\\|\eta_s\rangle\end{pmatrix}, \quad U(\phi) = \begin{pmatrix}\cos\phi & -\sin\phi\\ \sin\phi & \cos\phi\end{pmatrix}, \quad (2)$$

where ϕ is the mixing angle. In such a scheme, the decay constants in the quark-flavor basis simply follow the pattern of state mixing due to the OZI-rule [21], i.e.

$$\begin{pmatrix}f_\eta^q & f_\eta^s\\ f_{\eta'}^q & f_{\eta'}^s\end{pmatrix} = U(\phi){\rm diag}[f_q, f_s], \quad (3)$$

where the two basic decay constants f_q and f_s are defined by

$$f_i = 2\sqrt{3}\int_{k_\perp^2\le\mu_0^2}\frac{{\rm d}x{\rm d}^2k_\perp}{16\pi^3}\Psi_{\eta_i}(x,k_\perp), \quad (4)$$

with μ_0 the factorization scale, which is of order $\mathcal{O}(1\,{\rm GeV})$.

Useful constraints to determine the η–η' mixing angle can be derived by considering the two-photon decay of η and η'. The decay amplitudes of $\eta_s \to \gamma\gamma$ and $\eta_q \to \gamma\gamma$ have a Lorentz structure similar to that of $\pi^0 \to \gamma\gamma$ [36]:[1]

$$\mathcal{A}_{P\to\gamma_1(k_1)\gamma_2(k_2)} = \frac{\alpha}{\pi}\frac{c_P}{f_P}\epsilon^{\mu\nu\alpha\beta}\epsilon_\mu^*(k_1)\epsilon_\nu^*(k_2)k_{1\alpha}k_{2\beta}, \quad (5)$$

where the fine-structure constant $\alpha = 1/137$, $c_P = (c_s, c_q) = \left(\sqrt{2}/3, 5/3\right)$ for the states $P = (\eta_s, \eta_q)$, and f_P is the corresponding decay constant. Then the decay widths for $\eta \to \gamma\gamma$ and $\eta' \to \gamma\gamma$ can be written

$$\Gamma_{\eta\to\gamma\gamma} = \frac{\alpha^2M_\eta^3}{64\pi^3}\left(\frac{c_q\cos\phi}{f_q} - \frac{c_s\sin\phi}{f_s}\right)^2$$

and

$$\Gamma_{\eta'\to\gamma\gamma} = \frac{\alpha^2M_{\eta'}^3}{64\pi^3}\left(\frac{c_q\sin\phi}{f_q} + \frac{c_s\cos\phi}{f_s}\right)^2, \quad (6)$$

where the two-photon decay widths of η and η' and their masses can be found in PDG [37]; we have

$$\Gamma_{\eta\to\gamma\gamma} = 0.46 \pm 0.04\,{\rm keV}, \quad M_\eta = 547.30 \pm 0.12\,{\rm MeV},$$
$$\Gamma_{\eta'\to\gamma\gamma} = 4.37 \pm 0.25\,{\rm keV}, \quad M_{\eta'} = 957.78 \pm 0.14\,{\rm MeV}.$$

From (6), we obtain the correlation between f_q/f_s and ϕ:

$$f_q = \frac{c_q\alpha}{8\pi^{3/2}}\left[\sqrt{\frac{\Gamma_{\eta\to\gamma\gamma}}{M_\eta^3}}\cos\phi + \sqrt{\frac{\Gamma_{\eta'\to\gamma\gamma}}{M_{\eta'}^3}}\sin\phi\right]^{-1} \quad (7)$$

and

$$f_s = \frac{c_s\alpha}{8\pi^{3/2}}\left[\sqrt{\frac{\Gamma_{\eta'\to\gamma\gamma}}{M_{\eta'}^3}}\cos\phi - \sqrt{\frac{\Gamma_{\eta\to\gamma\gamma}}{M_\eta^3}}\sin\phi\right]^{-1}. \quad (8)$$

It shows that, knowing the range of the mixing angle ϕ, the ranges of the decay constants f_q and f_s can be determined accordingly, and vice versa.

[1] It is noted that the higher helicity states do not have a contribution to the decay amplitude.

2.2 A brief review of the $\pi\gamma$ transition form factor

In order to calculate the $\eta\gamma$ and $\eta'\gamma$ transition form factors, we first give a brief review of the $\pi\gamma$ transition form factor $F_{\pi\gamma}(Q^2)$. A comprehensive analysis of $F_{\pi\gamma}(Q^2)$ has been given in [32], in which the transverse-momentum dependence of both the hard-scattering amplitude and the LC wavefunction and the contributions beyond the leading Fock state have been taken into consideration. Especially, a phenomenological expression to estimate the contributions beyond the leading Fock state has been constructed, which is based on the form factors' asymptotic behavior at $Q^2 \to 0$ and $Q^2 \to \infty$.

As has been pointed out in [27], the transverse-momentum dependence of both the hard-scattering amplitude and the wavefunction of the meson should be kept to give a consistent analysis of the form factor. The revised LC harmonic oscillator model, as suggested in [38], was employed for the LC wavefunction $\Psi_\pi(x, \mathbf{k}_\perp)$, which is constructed based on the Brodsky–Huang–Lepage (BHL) prescription [30, 31]. More explicitly, the LC wavefunction of $\pi^0 = \frac{1}{\sqrt{2}}|u\bar{u} - d\bar{d}\rangle$ can be written as

$$\Psi_\pi(x, \mathbf{k}_\perp) = A_\pi \left[\exp\left(-\frac{\mathbf{k}_\perp^2 + m_q^2}{8{\beta_\pi}^2 x(1-x)}\right)\chi^K(m_q, x, \mathbf{k}_\perp)\right], \tag{9}$$

with the normalization constant A_π, the harmonic scale β_π and the light quark mass m_q to be determined. Since the contribution from the higher helicity states ($\lambda_1 + \lambda_2 = \pm 1$) has a small contribution in comparison to the usual helicity state ($\lambda_1 + \lambda_2 = 0$), we only write the explicit term for the usual helicity state. The spin-space wavefunction $\chi^K(x, \mathbf{k}_\perp)$ for the usual helicity state of the pion can be written [38] $\chi^K(m_q, x, \mathbf{k}_\perp) = m_q/\sqrt{m_q^2 + k_\perp^2}$, where $k_\perp = |\mathbf{k}_\perp|$. Furthermore, one can derive a relation between m_q and β_π by adopting the constraints from $\pi^0 \to \mu\nu$ and $\pi^0 \to \gamma\gamma$ [32]:

$$6.00\frac{m_q\beta_\pi}{f_\pi^2} \cong 1.12\left(\frac{m_q}{\beta_\pi} + 1.31\right)\left(\frac{m_q}{\beta_\pi} + 5.47 \times 10^1\right). \tag{10}$$

There are two basic types of contributions to $F_{\pi\gamma}(Q^2)$ [30–32], i.e.

$$F_{\pi\gamma}(Q^2) = F_{\pi\gamma}^{(V)}(Q^2) + F_{\pi\gamma}^{(NV)}(Q^2). \tag{11}$$

$F_{\pi\gamma}^{(V)}(Q^2)$ involves direct annihilation of a $(q\bar{q})$-pair into two photons, which is the leading Fock state contribution; it dominates the large Q^2 contribution. $F_{\pi\gamma}^{(NV)}(Q^2)$ involves the case of one-photon coupling 'inside' the LC wavefunction of the π meson, i.e. strong interactions occur among the photon interactions, which is related to the contributions of higher Fock states.

By keeping the transverse-momentum dependence in both the hard scattering amplitude and the LC wavefunction, the valence quark state transition form factor $F_{\pi\gamma}^{(V)}(Q^2)$ can be written as

$$F_{\pi\gamma}^{(V)}(Q^2) = 2\sqrt{3}e_\pi \int_0^1 [\mathrm{d}x] \int \frac{\mathrm{d}^2\mathbf{k}_\perp}{16\pi^3}\Psi_\pi(x, \mathbf{k}_\perp)T_H(x, x', \mathbf{k}_\perp), \tag{12}$$

where $[\mathrm{d}x] = \mathrm{d}x\mathrm{d}x'\delta(1-x-x')$, $e_\pi = (e_u^2 - e_d^2)$ and the hard-scattering amplitude $T_H(x, x', \mathbf{k}_\perp)$ takes the form

$$T_H(x, x', \mathbf{k}_\perp) = \frac{\mathbf{q}_\perp(x'\mathbf{q}_\perp + \mathbf{k}_\perp)}{\mathbf{q}_\perp^2(x'\mathbf{q}_\perp + \mathbf{k}_\perp)^2} + (x \leftrightarrow x').$$

$F_{\pi\gamma}^{(V)}(Q^2)$ can be further simplified, as the model wavefunction depends on $\mathbf{k}_\perp$ through $k_\perp^2$ only, i.e. $\Psi_\pi(x, \mathbf{k}_\perp) = \Psi_\pi(x, k_\perp^2)$, and we have

$$F_{\pi\gamma}^{(V)}(Q^2) = \frac{\sqrt{3}e_\pi}{4\pi^2}\int_0^1 \frac{\mathrm{d}x}{xQ^2}\int_0^{x^2Q^2}\Psi_\pi(x, k_\perp^2)\mathrm{d}k_\perp^2. \tag{13}$$

As for the second type of contribution, $F_{\pi\gamma}^{(NV)}(Q^2)$, it is difficult to calculate it in any Q^2 region due to its non-perturbative nature. One can construct a phenomenological model for $F_{\pi\gamma}^{(NV)}(Q^2)$, based on the asymptotic behavior at $Q^2 \to 0$ and $Q^2 \to \infty$. As suggested in [32], we assume that it takes the following form:

$$F_{\pi\gamma}^{(NV)}(Q^2) = \frac{\alpha}{(1 + Q^2/\kappa^2)^2}, \tag{14}$$

where κ and α are two parameters that are determined by the asymptotic behavior at $Q^2 \to 0$, i.e.

$$\alpha = \frac{1}{2}F_{\pi\gamma}(Q^2)|_{Q^2\to 0}$$

and

$$\kappa = \sqrt{-\frac{2\alpha}{\frac{\partial}{\partial Q^2}F_{\pi\gamma}^{(NV)}(Q^2)|_{Q^2\to 0}}}, \tag{15}$$

where the first derivative of $F_{\pi\gamma}^{(NV)}(Q^2)$ over Q^2 takes the form

$$F_{\pi\gamma}^{(NV)\prime}(Q^2)|_{Q^2\to 0} = \frac{\sqrt{3}e_\pi}{8\pi^2}\left[\frac{\partial}{\partial Q^2}\int_0^1\int_0^{x^2Q^2}\left(\frac{\Psi_\pi(x, k_\perp^2)}{x^2Q^2}\right)\mathrm{d}x\mathrm{d}k_\perp^2\right]_{Q^2\to 0}.$$

From the phenomenological formula (14), it is easy to find that $F_{\pi\gamma}^{(NV)}(Q^2)$ will be suppressed by $1/Q^2$ to $F_{\pi\gamma}^{(V)}(Q^2)$ in the limit $Q^2 \to \infty$.

2.3 $\eta\gamma$ and $\eta'\gamma$ transition form factors

As for the LC wavefunctions for the pseudoscalars, $\eta_q = \frac{1}{\sqrt{2}}|u\bar{u} + d\bar{d}\rangle$ and $\eta_s = |s\bar{s}\rangle$, they can be modeled as [38]

$$\Psi_{\eta_i}(x, \mathbf{k}_\perp) = A_i\left[\exp\left(-\frac{\mathbf{k}_\perp^2 + m_i^2}{8{\beta_i}^2 x(1-x)}\right)\chi^K(m_i, x, \mathbf{k}_\perp)\right], \tag{16}$$

where $i = q, s$ respectively. They also depend on $\mathbf{k}_\perp$ through $k_\perp^2$ only, i.e. $\Psi_{\eta_i}(x, \mathbf{k}_\perp) = \Psi_{\eta_i}(x, k_\perp^2)$. Substituting them into the normalization (3), we obtain

$$\int_0^1 \frac{A_i m_i \beta_i \sqrt{x(1-x)}}{4\sqrt{2}\pi^{3/2}} \times \left(\mathrm{Erf}\left[\sqrt{\frac{m_i^2+\mu_0^2}{8\beta_i^2 x(1-x)}} \right] - \mathrm{Erf}\left[\sqrt{\frac{m_i^2}{8\beta_i^2 x(1-x)}} \right] \right) \mathrm{d}x = \frac{f_i}{2\sqrt{3}}, \quad (17)$$

where μ_0 stands for the factorization scale, and following the discussion in [32], we take its value to be $\mu_0 \simeq 2\,\mathrm{GeV}$. With such a choice, one may safely set $\mu_0 \to \infty$ to simplify the computation, e.g. $\mathrm{Erf}\left[\sqrt{\frac{m_i^2+\mu_0^2}{8\beta_i^2 x(1-x)}} \right] |_{\mu_0 \to \infty} \to 1$, due to the fact that the contribution from the higher $|\mathbf{k}_\perp|$ region to the wavefunction normalization falls off exponentially for the above model wavefunctions.

Under the quark-flavor mixing scheme, the $\eta\gamma$ and $\eta'\gamma$ transition form factors take the following form:

$$F_{\eta\gamma}(Q^2) = F_{\eta_q\gamma}(Q^2)\cos\phi - F_{\eta_s\gamma}(Q^2)\sin\phi \quad (18)$$

and

$$F_{\eta'\gamma}(Q^2) = F_{\eta_q\gamma}(Q^2)\sin\phi + F_{\eta_s\gamma}(Q^2)\cos\phi\,, \quad (19)$$

where $F_{\eta_q\gamma}(Q^2)$ and $F_{\eta_s\gamma}(Q^2)$ stand for the $\eta_q\gamma$ and $\eta_s\gamma$ form factors, respectively. Similar to the pion–photon transition form factor, the pseudoscalar form factors $F_{P\gamma}(Q^2)$ ($P = \eta_q$ and η_s) can also be divided into the following two parts:

$$F_{P\gamma}(Q^2) = F_{P\gamma}^{(V)}(Q^2) + F_{P\gamma}^{(NV)}(Q^2)\,. \quad (20)$$

The leading Fock state contribution $F_{P\gamma}^{(V)}(Q^2)$ can be simplified like (13), and we only need to replace e_π and Ψ_π to the present case of e_P and Ψ_P, where $e_P = (e_u^2 + e_d^2, \sqrt{2}e_s^2)$ for $P = (\eta_q, \eta_s)$ respectively. And similar to (14), we assume the following form for the power suppressed non-leading Fock state contribution $F_{P\gamma}^{(NV)}(Q^2)$:

$$F_{P\gamma}^{(NV)}(Q^2) = \frac{\alpha}{(1+Q^2/\kappa^2)^2}\,, \quad (21)$$

where κ and α are two parameters that are determined by

$$\alpha = \frac{1}{2} F_{P\gamma}(Q^2)|_{Q^2\to 0}\,, \qquad \kappa = \sqrt{-\frac{2\alpha}{\frac{\partial}{\partial Q^2} F_{P\gamma}^{(NV)}(Q^2)\Big|_{Q^2\to 0}}}\,, \quad (22)$$

where the first derivative of $F_{P\gamma}^{(NV)}(Q^2)$ over Q^2 takes the form

$$F_{P\gamma}^{(NV)'}(Q^2)|_{Q^2\to 0} = \frac{\sqrt{3}e_P}{8\pi^2}\left[\frac{\partial}{\partial Q^2} \int_0^1 \int_0^{x^2Q^2} \left(\frac{\Psi_P(x, k_\perp^2)}{x^2 Q^2} \right) \mathrm{d}x \mathrm{d}k_\perp^2 \right]_{Q^2\to 0}.$$

Naively, under strict $\mathrm{SU}(3)_F$ symmetry, one has $F_{\eta_q\gamma}(Q^2) \cong F_{\eta_s\gamma}(Q^2)$, which leads to

$$F_{\eta\gamma}(Q^2) \propto \cos(\phi + 45^\circ) \text{ and } F_{\eta'\gamma}(Q^2) \propto \sin(\phi + 45^\circ)\,. \quad (23)$$

Therefore, if ϕ varies within the region of $[0, 45^\circ]$, which is most probably the case, $F_{\eta\gamma}(Q^2)$ under SU(3) will decrease with increasing ϕ, while $F_{\eta'\gamma}(Q^2)$ will also increase with ϕ. In the next section, we will show that in the case of broken $\mathrm{SU}(3)_F$ symmetry, this is still a fact. And then the possible range of ϕ can be obtained by comparing with the experimental data on the transition form factors $F_{\eta\gamma}(Q^2)$ and $F_{\eta'\gamma}(Q^2)$.

3 Numerical analysis

With the help of the constraints from the two-photon decay amplitudes of η and η' (e.g. (7) and (8)) and the experimental data on the $\eta\gamma$ and $\eta'\gamma$ transition form factors [5–9], one can obtain a reasonable region for ϕ. There are several parameters in the wavefunction Ψ_P to be determined. As for the constituent quark masses, we take the conventional values: $m_{u,d} = 300\,\mathrm{MeV}$ and $m_s = 450\,\mathrm{MeV}$. By studying the pion–photon transition form factor, one may observe that the best fit of the experimental data is derived in the case of $m_{u,d} \simeq 300\,\mathrm{MeV}$ [32]. For the transverse parameters β_π, β_q and β_s, they are proportional to the inverses of the charge radii of the corresponding valence quark states [39]. The differences between them are less than $\sim 10\%$, as shown in [40]. For simplicity, we assume $\beta_q = \beta_s = \beta_\pi$ throughout this work. The uncertainties from the different choices of β_q, β_s, $m_{u,d}$ and m_s will be discussed in Sect. 4.

As for the experimental results of $F_{\eta\gamma}(Q^2)$ and $F_{\eta'\gamma}(Q^2)$, we take the pole-mass parameter fit formula that is adopted in those experiments [5–9]:

$$Q^2 F_{(\eta/\eta')\gamma}(Q^2) = \frac{1}{(4\pi\alpha)^2}\sqrt{\frac{64\pi\Gamma\left[(\eta/\eta')\to\gamma\gamma\right]}{M_P^3}}\frac{Q^2}{1+Q^2/\Lambda_P^2}\,. \quad (24)$$

As for the values of Λ_η and $\Lambda_{\eta'}$, we have

$$\Lambda_\eta = 774 \pm 11 \pm 16 \pm 22\,\mathrm{MeV}\,, \quad \Lambda_{\eta'} = 859 \pm 9 \pm 18 \pm 20\,\mathrm{MeV} \quad (25)$$

for the CLEO collaboration [5, 6];

$$\Lambda_\eta = 0.70 \pm 0.08\,\mathrm{GeV}\,, \quad \Lambda_{\eta'} = 0.85 \pm 0.07\,\mathrm{GeV} \quad (26)$$

for the TPC/Two-Gamma collaboration [8];

$$\Lambda_{\eta'} = 900 \pm 46 \pm 22\,\mathrm{MeV} \quad (27)$$

for the L3 collaboration [9], and

$$\Lambda_\eta = 0.84 \pm 0.06\,\mathrm{GeV}\,, \Lambda_{\eta'} = 0.79 \pm 0.04\,\mathrm{GeV} \quad (28)$$

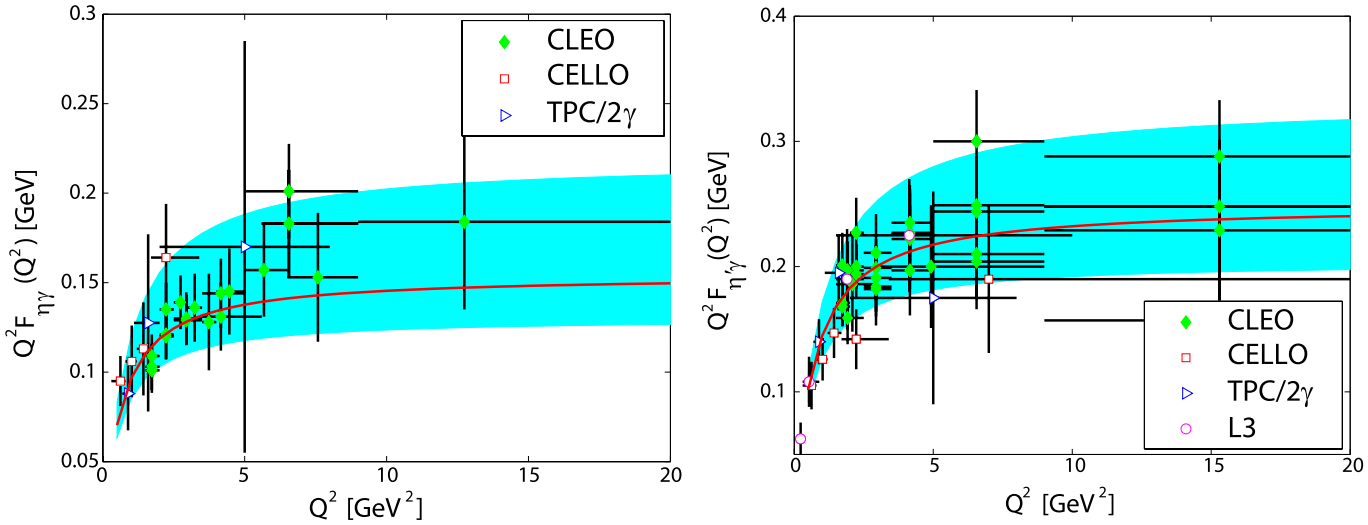

Fig. 1. Color on-line: Pole-mass fit of $Q^2F_{\eta\gamma}(Q^2)$ (*left*) and $Q^2F_{\eta'\gamma}(Q^2)$ (*right*) from the experimental data [5–9]. The *solid line* stands for the average pole-mass fit with $\bar{\Lambda}_\eta = 771$ MeV or $\bar{\Lambda}_{\eta'} = 850$ MeV and the *shaded band* shows the experimental uncertainty

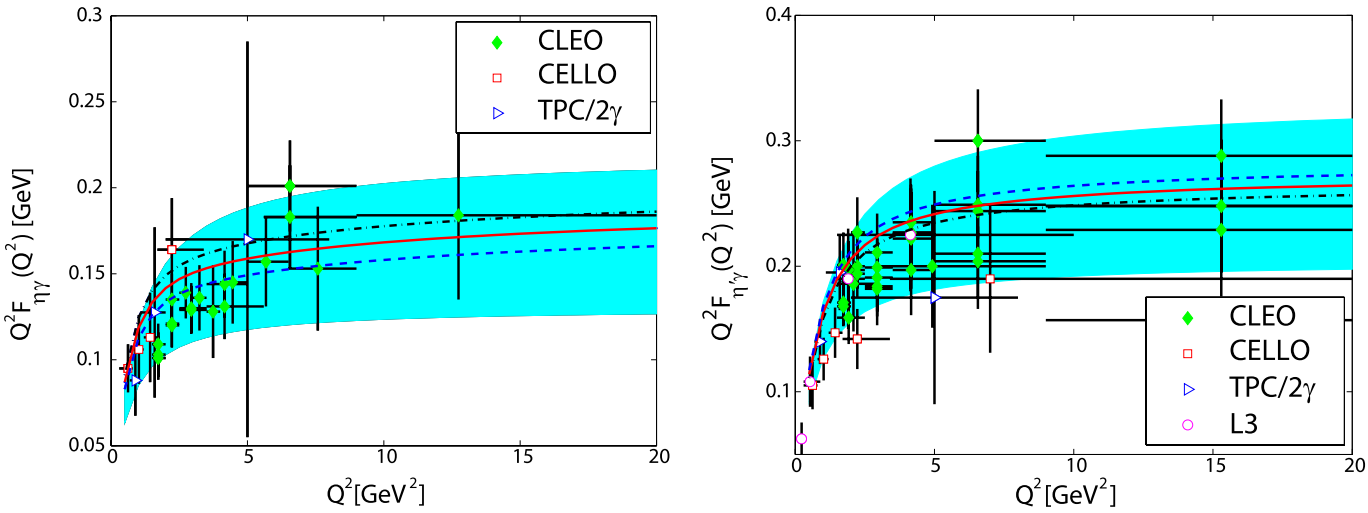

Fig. 2. Color on-line: $Q^2F_{\eta\gamma}(Q^2)$ and $Q^2F_{\eta'\gamma}(Q^2)$ with the BHL-like wavefunction. The *dash-dot line*, the *solid line* and the *dashed line* are for $\phi = 37.0°$, $\phi = 38.0°$ and $\phi = 39.0°$, respectively. It shows that $Q^2F_{\eta\gamma}(Q^2)$ decreases and $Q^2F_{\eta'\gamma}(Q^2)$ increases with increasing ϕ. The *shaded band* is the region allowed by the experiments [5–9]

for the CELLO collaboration [7]. Averaging the above experimental values, we obtain the central values for Λ_η and $\Lambda_{\eta'}$, i.e. $\bar{\Lambda}_\eta = 771$ MeV and $\bar{\Lambda}_{\eta'} = 850$ MeV. We draw the pole-mass fit of the form factors $Q^2F_{\eta\gamma}(Q^2)$ and $Q^2F_{\eta'\gamma}(Q^2)$ in Fig. 1, where the shaded band is derived by adopting the pole-mass fit formula (24) and by varying Λ_η and $\Lambda_{\eta'}$ within the widest possible range allowed by the above experimental results.[2] The shaded band (region) for $Q^2F_{\eta\gamma}(Q^2)$ and $Q^2F_{\eta'\gamma}(Q^2)$ can be regarded as constraints to determine the η/η' wavefunctions, i.e. the values of the parameters in the wavefunctions and also the mixing angle ϕ should take $Q^2F_{\eta\gamma}(Q^2)$ and $Q^2F_{\eta'\gamma}(Q^2)$ to within the region of the shaded bands as shown in Fig. 1.

From (17), we obtain

$$A_q \simeq 2.77 \times 10^2 f_q \text{ and } A_s \simeq 2.85 \times 10^2 f_s\,,$$

and then with the help of (7), (8), (18) and (19), it can be found that only the mixing angle ϕ is undetermined. As shown in Fig. 2, one may observe that the value of $Q^2F_{\eta\gamma}(Q^2)$ decreases with increasing ϕ, while the value of $Q^2F_{\eta'\gamma}(Q^2)$ increases, and such a fact can be used to determine the possible range for ϕ by comparing with the experimental data. In fact, it can be found that the lower limit of ϕ is determined by $Q^2F_{\eta\gamma}(Q^2)$, and the upper limit

[2] Here we do not take the weighted average of these experiments and treat them on an equal footing, as these experiments concentrate on different energy regions and only a few data are available.

of ϕ is determined by $Q^2F_{\eta'\gamma}(Q^2)$, i.e.

$$\phi \cong 38.0^\circ \pm 1.0^\circ\,. \tag{29}$$

Furthermore, we obtain $\frac{f_q}{f_\pi} = 1.07 \pm 0.01$ and $\frac{f_s}{f_\pi} = 1.24 \pm 0.10$. By using the correlation between the quark-flavor mixing scheme and the octet–singlet scheme [21, 33], we obtain

$$\theta_P = \phi - \arctan\sqrt{2} = -17.0^\circ \pm 1.0^\circ\,, \tag{30}$$

$$\theta_8 = \phi - \arctan\frac{\sqrt{2}f_s}{f_q} = -20.7^\circ \pm 1.0^\circ\,,$$

$$\theta_1 = \phi - \arctan\frac{\sqrt{2}f_q}{f_s} = -12.6^\circ \pm 3.3^\circ \tag{31}$$

and

$$\frac{f_8}{f_\pi} = \sqrt{\frac{f_q^2+2f_s^2}{3}}\Bigg/ f_\pi = 1.19 \pm 0.07\,,$$

$$\frac{f_1}{f_\pi} = \sqrt{\frac{2f_q^2+f_s^2}{3}}\Bigg/ f_\pi = 1.13 \pm 0.03\,. \tag{32}$$

4 Discussion of the uncertainties in determining ϕ

In this section, we discuss the uncertainties in determining the mixing angle ϕ from the above approach. First, we compare the differences caused by the different model wavefunctions, e.g. the BHL-like one and the CZ-like (Chernyak–Zhitnitsky-like) one [41] which is much broader. Next, we restrict ourselves to the use of the BHL-like model wavefunction for a detailed analysis of the effects on the determination of ϕ caused by each of the uncertainty sources separately, where the uncertainty sources mainly include the value of β_q and β_s, the masses of the constitutent quarks u/d and s, and the possible intrinsic charm components of η and η'. Some other even smaller uncertainty sources for the electro-magnetic transition form factors such as the gluon component in η/η' will not be discussed.[3]

4.1 Model dependence

One possible typical broad wavefunction is described by the CZ-like wavefunction. For convenience and for simplicity, we take $m_q = 0.30\,\mathrm{GeV}$ and $m_s = 0.45\,\mathrm{GeV}$, and $\beta_q = \beta_s = \beta_\pi$. It can be found that $\beta_\pi = 0.70\,\mathrm{GeV}$ for the case of the CZ-like wavefunction [32].

The CZ-like wavefunctions for η_q and η_s take the form

$$\Psi_{\eta_i}^{\mathrm{CZ}}(x,\mathbf{k}_\perp) = A_i^{\mathrm{CZ}}(1-2x)^2 \times\left[\exp\left(-\frac{\mathbf{k}_\perp^2+m_i^2}{8\beta_i^2 x(1-x)}\right)\chi^K(m_i,x,\mathbf{k}_\perp)\right], \tag{33}$$

where $i = q, s$. Following a similar procedure, it can be found that

$$A_q^{\mathrm{CZ}} \simeq 8.86\times 10^2 f_q\,, \quad \text{and} \quad A_s^{\mathrm{CZ}} \simeq 8.95\times 10^2 f_s\,.$$

By a numerical calculation, it can be found that the $\eta\gamma$ and $\eta'\gamma$ transition form factors from the CZ-like wavefunction increase faster than the case of the BHL-like wavefunction. The shapes of the $\eta\gamma$ and $\eta'\gamma$ form factors from the BHL-like wavefunction are closer to the pole-mass parameter fits of the experimental data. Although the model is different, one may find that the value of $Q^2F_{\eta\gamma}(Q^2)$ decreases with increasing ϕ, while the value of $Q^2F_{\eta'\gamma}(Q^2)$ increases. Therefore, the range for ϕ can also be estimated, i.e. $\phi \cong 38.0^\circ \pm 1.0^\circ$, which is close to the case of the BHL-like wavefunction. This shows that the η–η' mixing angle ϕ is almost model independent in our approach.

Recently, the BaBar collaboration has measured the value of $Q^2F_{\eta\gamma}(Q^2)$ and $Q^2F_{\eta'\gamma}(Q^2)$ at $Q^2 = 112\,\mathrm{GeV}^2$ [12]: $Q^2F_{\eta\gamma}(Q^2) = 0.229 \pm 0.030 \pm 0.008\,\mathrm{GeV}$ and $Q^2F_{\eta'\gamma}(Q^2) = 0.251 \pm 0.019 \pm 0.008\,\mathrm{GeV}$, and the ratio of the form factors

$$\kappa = \left.\frac{Q^2F_{\eta'\gamma}(Q^2)}{Q^2F_{\eta\gamma}(Q^2)}\right|_{Q^2=112\ \mathrm{GeV}^2} = 1.10 \pm 0.17\,.$$

In the case of $\phi \in [37^\circ, 39^\circ]$, for the BHL-like wavefunction, we have $Q^2F_{\eta\gamma}(Q^2) = [0.176, 0.190]\,\mathrm{GeV}$ and $Q^2F_{\eta'\gamma}(Q^2) = [0.228, 0.277]\,\mathrm{GeV}$ at $Q^2 = 112\,\mathrm{GeV}^2$, which is close to the experimental values[4] and leads to $\kappa = 1.44 \pm 0.06.$, while for the CZ-like wavefunction we have $Q^2F_{\eta\gamma}(Q^2) = [0.267, 0.297]\,\mathrm{GeV}$ and $Q^2F_{\eta'\gamma}(Q^2) = [0.388, 0.411]\,\mathrm{GeV}$ at $Q^2 = 112\,\mathrm{GeV}^2$, which is somewhat bigger than the experimental values and leads to $\kappa = 1.41 \pm 0.06$. For comparison, one may conclude that the asymptotic behavior of the form factors $Q^2F_{\eta\gamma}(Q^2)$ and $Q^2F_{\eta'\gamma}(Q^2)$ disfavor the CZ-like wavefunction but favor the asymptotic-like wavefunction.

It is due to these differences that the form factors of the CZ-like wavefunction and the BHL-like one are affected differently by the following uncertainty sources. For example, as shown in [32], the best fit of the $\pi\gamma$ form factor to the experimental data is obtained with $m_q \simeq 300\,\mathrm{MeV}$ in the case of the BHL-like wavefunction, which is shifted to $m_q \simeq 400\,\mathrm{MeV}$ for the case of the CZ-like wavefunction.

In the following, we will only take the BHL-like wavefunction as an explicit example to show the uncertainties; the case of the CZ-like one can be done in a similar way. For clarity, in studying the uncertainty caused by a certain source, the other uncertainty sources are taken to have their central values, as adopted above.

[3] The gluon contributions might be important to some other exclusive processes like two-body non-leptonic exclusive decays for the B meson. A discussion of the two-gluon components in the form factors can be found in [42].

[4] It is also close to the theoretical predictions based on the asymptotic wavefunction that have been shown clearly in Fig. 13 of [12].

4.2 The uncertainty $\Delta\phi^m$ from m_q and m_s

We take a wider range for m_q and m_s to study their effects on the mixing angle ϕ, e.g. $m_q = 0.30 \pm 0.10\,\text{GeV}$ and $m_s = 0.45 \pm 0.10\,\text{GeV}$. In the present case we adopt $\beta_p = \beta_s = \beta_\pi$, where the value of β_π varies within the region of $[0.48, 0.70]\,\text{GeV}$ according to the value of m_q [32]. From (17), we obtain the uncertainty from the constituent quark masses:

$$A_p \simeq 2.77^{+1.00}_{-0.48} \times 10^2 f_p\,, \quad A_s \simeq 2.85^{+1.99}_{-1.10} \times 10^2 f_s\,,$$

where both A_p and A_s increase with the increment of m_q and m_s respectively. Also, it can be found numerically that

$$\Delta\phi^m \leq \pm 0.5^\circ\,. \tag{34}$$

4.3 The uncertainty $\Delta\phi^\beta$ from β_q and β_s

Due to SU(3) symmetry breaking, there are differences among β_π, β_q and β_s, which are smaller than 10%, as can be seen by a light-cone quark model analysis [40]. For clarity, we choose the broader ranges of $\beta_q = 0.55 \pm 0.10\,\text{GeV}$ and $\beta_s = 0.55 \pm 0.10\,\text{GeV}$ to discuss how these transverse size parameters affect the mixing angle. Other wavefunction parameters are fixed by setting $m_q = 0.30\,\text{GeV}$ (or equivalently $\beta_\pi = 0.55\,\text{GeV}$) and $m_s = 0.45\,\text{GeV}$. Under such conditions, we have the following uncertainty from the transverse parameters β_q and β_s:

$$A_p \simeq 2.77^{+1.31}_{-0.69} \times 10^2 f_p\,, \quad A_s \simeq 2.85^{+1.94}_{-0.89} \times 10^2 f_s\,,$$

where both A_p and A_s increase with the decreasing β_p and β_s, respectively. It can be found numerically that

$$\Delta\phi^\beta \leq \pm 2.0^\circ\,. \tag{35}$$

4.4 The uncertainty $\Delta\phi^c$ from the intrinsic charm component

It has been suggested that a larger intrinsic charm component might be possible, explaining the abnormally large production of η' in the standard model [43, 44]. However, some studies in the literature disfavor such a large intrinsic charm component; see e.g. [19, 24, 45, 46] and references therein. It has been found [19] that the mixing between the $c\bar{c}$ state with a $q\bar{q}$–$s\bar{s}$ basis is quite small, e.g. less than 2%. So, for simplicity, we do not consider the mixing between a $c\bar{c}$ and a $q\bar{q}$–$s\bar{s}$ basis. We then have

$$F_{\eta\gamma}(Q^2) = F_{\eta_q\gamma}(Q^2)\cos\phi - F_{\eta_s\gamma}(Q^2)\sin\phi + F^{\eta}_{\eta_c\gamma}(Q^2)\,, \tag{36}$$

$$F_{\eta'\gamma}(Q^2) = F_{\eta_q\gamma}(Q^2)\sin\phi + F_{\eta_s\gamma}(Q^2)\cos\phi + F^{\eta'}_{\eta_c\gamma}(Q^2)\,, \tag{37}$$

where $F^{\eta}_{\eta_c\gamma}(Q^2)$ and $F^{\eta'}_{\eta_c\gamma}(Q^2)$ correspond to the contributions from the intrinsic charm component in η and η', respectively, which will be calculated in the following.

The wavefunction of the "intrinsic" charm component $\eta_c = |c\bar{c}\rangle$ can be modeled by

$$\Psi^c_{\eta/\eta'}(x, \mathbf{k}_\perp) = A^c_{\eta/\eta'}\left[\exp\left(-\frac{\mathbf{k}^2_\perp + m_c^2}{8{\beta_c}^2 x(1-x)}\right)\chi^K(m_c, x, \mathbf{k}_\perp)\right], \tag{38}$$

where we adopt $\beta_c = \beta_\pi = 0.55\,\text{GeV}$ and $m_c = 1.5\,\text{GeV}$.[5] The overall factor $A^c_{\eta/\eta'}$ is determined by a wavefunction normalization similar to (17), which shows that

$$A^c_\eta = 9.45 \times 10^3 f^c_\eta\,, \quad A^c_{\eta'} = 9.45 \times 10^3 f^c_{\eta'}\,,$$

where f^c_η and $f^c_{\eta'}$ are related by [19],

$$\frac{f^c_\eta}{f^c_{\eta'}} = -\tan\left[\phi - \arctan\frac{\sqrt{2}f_s}{f_q}\right] \tag{39}$$

and on taking $\phi = 38.0^\circ \pm 1.0^\circ$, we have $\frac{f^c_\eta}{f^c_{\eta'}} = [0.36, 0.40]$.

It is noted that different from the $\eta_q\gamma$ and $\eta_s\gamma$ transition form factors, the helicity-flip amplitude, which is proportional to the current quark mass, cannot be ignored for the present case. For the $\eta_c\gamma$ transition form factor, a direct calculation shows[6] that

$$F^{\eta/\eta'}_{\eta_c\gamma}(Q^2) = 2\sqrt{6}e_c^2\int_0^1 [\mathrm{d}x] \times \int \frac{\mathrm{d}^2\mathbf{k}_\perp}{16\pi^3}\Psi^c_{\eta/\eta'}(x, \mathbf{k}_\perp)T^c_H(x, x', \mathbf{k}_\perp)\,. \tag{40}$$

where the hard-scattering amplitude $T^c_H(x, x', \mathbf{k}_\perp)$, which includes all the helicity states ($\lambda_1 + \lambda_2 = 0, \pm 1$) of η_c takes the form [24, 47],

$$T^c_H(x, x', \mathbf{k}_\perp) = \frac{\mathbf{q}_\perp(x'\mathbf{q}_\perp + \mathbf{k}_\perp)}{\mathbf{q}^2_\perp[(x'\mathbf{q}_\perp + \mathbf{k}_\perp)^2 + m_c^2]} + (x \leftrightarrow x')\,. \tag{41}$$

The above formula can be further simplified by doing the integration over the azimuthal angle:

$$F_{\eta_c\gamma}(Q^2) = \frac{\sqrt{6}e_c^2}{4\pi^2}\int_0^1 \frac{\mathrm{d}x}{xQ^2}\int_0^\infty \Psi^c_{\eta/\eta'}(x, k^2_\perp) \times \left[1 + \frac{1 - z - y^2}{\sqrt{(z + (1-y)^2)(z + (1+y)^2)}}\right] k_\perp \mathrm{d}k_\perp\,, \tag{42}$$

where $z = \frac{m_c^2}{x^2Q^2}$ and $y = \frac{k_\perp}{xQ}$.

[5] By varying β_c and m_c within their possible regions, the following results will be only slightly changed, and the present conceptual results stay the same.

[6] We will not consider the contribution of the non-valence charm quark states, since it is quite small due to the large charm mass effect.

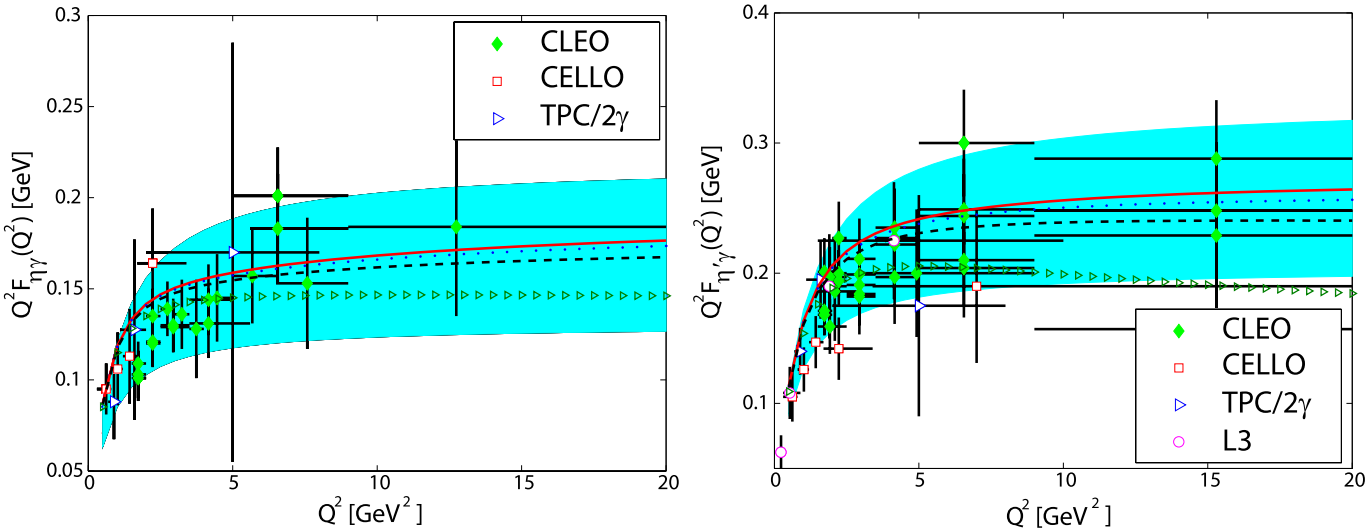

Fig. 3. $Q^2F_{\eta\gamma}(Q^2)$ and $Q^2F_{\eta'\gamma}(Q^2)$ for $\phi = 38.0^\circ$ with the BHL-like wavefunction. The *shaded band* shows the experimental uncertainty [5–9]. The *solid line*, the *dotted line*, the *dashed line* and the *triangle line* are for $f_{\eta'}^c = 0$, -5 MeV, -15 MeV and -50 MeV, respectively

Taking $\phi = 38.0^\circ$, we show in Fig. 3 how the value of $f_{\eta'}^c$ affects the form factors $Q^2F_{\eta\gamma}(Q^2)$ and $Q^2F_{\eta'\gamma}(Q^2)$. One may observe that the experimental data disfavor a larger charm component: $|f_{\eta'}^c| > 50$ MeV. Or conversely, it can be founded that under the condition of $|f_{\eta'}^c| \leq 50$ MeV, the uncertainty from the possible intrinsic charm components is given by

$$\Delta\phi^c \leq \pm 1^\circ\,. \tag{43}$$

4.5 A summary remark on ϕ

Under the quark-flavor mixing scheme, and by carefully dealing with the contributions of the higher Fock states, the possible range for ϕ can be derived by comparing with the experimental data on the form factors $F_{\eta\gamma}(Q^2)$ and $F_{\eta'\gamma}(Q^2)$, due to the fact that the value of $Q^2F_{\eta\gamma}(Q^2)$ decreases, while the value of $Q^2F_{\eta'\gamma}(Q^2)$ increases, with increasing ϕ in the whole Q^2 region. It has been found that the allowed range for the mixing angle ϕ is

$$\phi \cong 38.0^\circ \pm 1.0^\circ \pm 2.0^\circ\,, \tag{44}$$

where the first error is from the experimental uncertainty [5–9] and the second error is from the uncertainties of the wavefunction parameters and the possible intrinsic charm component in η and η'. It should be noted that the second uncertainty is lower than the direct sum of the errors caused by each source separately, i.e. $\Delta\phi^m + \Delta\phi^\beta + \Delta\phi^c$, which is due to the fact that these uncertainty sources are correlated to each other.

5 Summary

In the present paper, we have performed a light-cone pQCD analysis of the $\eta\gamma$ and $\eta'\gamma$ transition form factors $F_{\eta\gamma}(Q^2)$ and $F_{\eta'\gamma}(Q^2)$ involving the transverse-momentum corrections, in which η–η' mixing effects and the contributions beyond the leading Fock state have been taken in consideration. For this purpose, we have adopted the quark-flavor mixing scheme for η and η' mixing, and we have constructed a phenomenological expression to estimate the contributions beyond the leading Fock state based on its asymptotic behavior at $Q^2 \to 0$ and $Q^2 \to \infty$. It has been found that the value of $Q^2F_{\eta\gamma}(Q^2)$ decreases, while the value of $Q^2F_{\eta'\gamma}(Q^2)$ increases, with increasing ϕ, in the whole Q^2 region, and thus the possible range for ϕ can be determined by comparing with the experimental data, which is found to be $\phi \cong 38.0^\circ \pm 1.0^\circ \pm 2.0^\circ$, with the first error coming from experimental uncertainty [5–9] and the second error from the uncertainties of the wavefunction parameters and the possible intrinsic charm component in η and η'. A more accurate weighted average of the above mentioned value together with the seven adopted experimental values as described in [19], and the two new experimental values, $\phi = 41.2^\circ \pm 1.2^\circ$ [14] and $\phi = 38.8^\circ \pm 1.2^\circ$ [15], yields $\bar{\phi} = 39.5^\circ \pm 0.5^\circ$. Furthermore, our results show that the η–η' mixing angle ϕ slightly depends on the different wavefunction models. However, the asymptotic behavior of the form factors $Q^2F_{\eta\gamma}(Q^2)$ and $Q^2F_{\eta'\gamma}(Q^2)$ disfavor the CZ-like wavefunction but favor the asymptotic-like wavefunction. It has been found that the intrinsic charm component in η and η' cannot be too big; e.g. $|f_{\eta'}^c| < 50$ MeV. Such a conclusion agrees with other investigations [19, 24, 45, 46]. These results are helpful to understand other exclusive processes involving the pseudo-scales η and η'.

Acknowledgements. This work was supported in part by the Natural Science Foundation of China (NSFC). Xing-Gang Wu thanks for the support from the China Postdoctoral Science Foundation.

References

1. G.P. Lepage, S.J. Brodsky, Phys. Rev. D **22**, 2157 (1980)
2. S.J. Brodsky, G.P. Lepage, Phys. Rev. D **24**, 1808 (1981)
3. G.P. Lepage, S.J. Brodsky, T. Huang, P.B. Mackezie, in Particles and Fields-2, page 83, Invited talk presented at the Banff summer Institute on Particle Physics, Banff, Alberta, Canada, 1981
4. S.J. Brodsky, H.C. Pauli, S.S. Pinsky, Phys. Rep. **301**, 299 (1998) and references therein
5. CLEO Collaboration, V. Savinov et al., hep-ex/9707028
6. CLEO Collaboration, J. Gronberg et al., Phys. Rev. D **57**, 33 (1998)
7. CELLO Collaboration, H.-J. Behrend et al., Z. Phys. C **49**, 401 (1991)
8. TPC/Two-Gamma Collaboration, H. Aihara et al., Phys. Rev. Lett. **64**, 172 (1990)
9. L3 Collaboration, M. Acciarri et al., Phys. Lett. B **418**, 399 (1998)
10. KLOE Collaboration, A. Aloisio et al., Phys. Lett. B **541**, 45 (2002)
11. KLOE Collaboration, S.E. Muller et al., Int. J. Mod. Phys. A **20**, 1888 (2005)
12. BABAR Collaboration, B. Aubert et al., Phys. Rev. D **74**, 012002 (2006)
13. PLUTO Collaboration, C. Berger et al., Phys. Lett. B **142**, 225 (1984)
14. P. Kroll, Mod. Phys. Lett. A **20**, 2667 (2005)
15. BES Collaboration, M. Ablikim et al., Phys. Rev. D **73**, 052008 (2006)
16. H. Fritzsch, J.D. Jackson, Phys. Lett. B **66**, 365 (1977)
17. N. Isgur, Phys. Rev. D **13**, 122 (1976)
18. F.J. Gilman, R. Kauffman, Phys. Rev. D **36**, 2761 (1987)
19. T. Feldmann, P. Kroll, B. Stech, Phys. Rev. D **58**, 114006 (1998)
20. T. Feldmann, P. Kroll, B. Stech, Phys. Lett. B **449**, 339 (1999)
21. T. Feldmann, Int. J. Mod. Phys. A **15**, 159 (2000)
22. T. Feldmann, P. Kroll, Eur. Phys. J. C **5**, 327 (1998)
23. J. Schechter, A. Subbaraman, H. Weigel, Phys. Rev. D **48**, 339 (1993)
24. J. Cao, F.G. Cao, T. Huang, B.Q. Ma, Phys. Rev. D **58**, 113006 (1998)
25. K. Kawarabayashi, N. Ohta, Nucl. Phys. B **175**, 477 (1980)
26. K. Kawarabayashi, Prog. Theor. Phys. **66**, 1789 (1981)
27. F.G. Cao, T. Huang, B.Q. Ma, Phys. Rev. D **53**, 6582 (1996)
28. R. Jakob, P. Kroll, M. Raulfs, J. Phys. G **22**, 45 (1996)
29. F.G. Cao, A.I. Signal, Phys. Rev. D **60**, 114012 (1999)
30. S.J. Brodsky, T. Huang, G.P. Lepage, in Particles and Fields-2, Proceedings of the Banff Summer Institute, Banff, Alberta, 1981, ed. by A.Z. Capri, A.N. Kamal (Plenum, New York, 1983), p. 143
31. T. Huang, in Proceedings of XXth International Conference on High Energy Physics (Madison, Wisconsin, 1980) ed. by L. Durand, L.G. Pondrom, AIP Conf. Proc. No. 69 (AIP, New York, 1981), p. 1000
32. T. Huang, X.G. Wu, hep-ph/0606135
33. T. Feldmann, Nucl. Phys. Proc. Suppl. **74**, 151 (1999)
34. H. Leutwyler, Nucl. Phys. Proc. Suppl. **64**, 223 (1998)
35. R. Kaiser, H. Leutwyler, hep-ph/9806336
36. J.F. Donoghue, B.R. Holstein, Y.-C.R. Lin, Phys. Rev. Lett. **16**, 2766 (1985)
37. Particle Data Group, E.J. Weinberg et al., Phys. Rev. D **66**, 010001 (2002)
38. T. Huang, B.Q. Ma, Q.X. Shen, Phys. Rev. D **49**, 1490 (1994)
39. T. Huang, X.G. Wu, Phys. Rev. D **70**, 053007 (2004)
40. H.M. Choi, C.R. Ji, Phys. Rev. D **59**, 074015 (1999)
41. V.L. Chernyak, A.R. Zhitnitsky, Nucl. Phys. B **201**, 492 (1982)
42. S.S. Agaev, N.G. Stefanis, Phys. Rev. D **70**, 054020 (2004)
43. I. Halperin, A. Zhitnitsky, Phys. Rev. D **56**, 7247 (1997)
44. H.Y. Cheng, B. Tseng, Phys. Lett. B **415**, 263 (1997)
45. T.W. Yeh, Phys. Rev. D **65**, 094019 (2002)
46. F. Yuan, K.-T. Chao, Phys. Rev. D **56**, 2495 (1997)
47. F.G. Cao, T. Huang, Phys. Rev. D **59**, 093004 (1999)